Solid State Phenomena
ISSN: 1662-9779, Vol. 342, pp 105-112
doi:10.4028/p-09h52t

Submitted: 2022-09-02
Revised: 2022-12-13
Accepted: 2022-12-13
Online: 2023-05-25

Quality Evaluation of 150 mm 4H-SiC Grown at over 1.5 mm/h by High-Temperature Chemical Vapor Deposition Method

Takeshi Okamoto[1,a *], Hideyuki Uehigashi[1,b], Takahiro Kanda[1,c], Nobuyuki Ohya[1,d], Akiyoshi Horiai[1,e], Soma Sakakibara[1,f], Takashi Kanemura[1,g], Kiyoshi Betsuyaku[2,h], Norihiro Hoshino[2,i], Isaho Kamata[2,j] and Hidekazu Tsuchida[2,k]

[1]MIRISE Technologies Corporation,
500-1 Minamiyama, Komenoki-cho, Nisshin-shi, Aichi 470-0111, Japan

[2]Central Research Institute of Electric Power Industry (CRIEPI),
2-6-1 Nagasaka, Yokosuka-shi, Kanagawa 240-0196, Japan

[a]takeshi.okamoto.j7a@mirise-techs.com, [b]hideyuki.uehigashi.j2f@mirise-techs.com
[c]takahiro.kanda.j2y@mirise-techs.com, [d]nobuyuki.oya.j5v@mirise-techs.com,
[e]akiyoshi.horiai.j7h@mirise-techs.com, [f]soma.sakakibara.j7b@mirise-techs.com,
[g]takashi.kanemura.j4y@mirise-techs.com, [h]betuyaku@criepi.denken.or.jp,
[i]nhoshino@criepi.denken.or.jp, [j]kamata@criepi.denken.or.jp, [k]tsuchida@criepi.denken.or.jp

Keywords: crystal growth, fast growth, crystal quality, high-temperature chemical vapor deposition method, HTCVD

Abstract. To reduce manufacturing costs, high-quality 150 mm 4H-SiC wafers were grown at over 1.5 mm/h by high-temperature chemical vapor deposition. The dislocations in the initial growth stage did not increase compared with those in the seed crystal. The dislocation densities decreased during crystal growth, and the densities of threading dislocations and basal plane dislocations at the growth thickness of 7.1 mm were 1186 and 211 /cm^2, respectively. The resolved shear stress, which is the cause of the increase in dislocations during growth, was calculated based on thermal fluid simulations; the shear stress of the grown crystal with a flat surface was small compared with that of the convex-shaped crystal. The dislocations did not increase likely because the crystals grown at high speeds were relatively flat. In addition, the decrease in dislocations was attributed to the frequent annihilation of dislocations due to the growth at a high temperature (2490 °C).

Introduction

Silicon carbide (SiC) is a wide-bandgap semiconductor material with a high breakdown electric field and high thermal conductivity. These excellent properties enable SiC power devices to achieve low power consumption, high breakdown voltage, and high-speed switching. The low manufacturing efficiency of SiC wafers limits the widespread use of SiC devices. Currently, almost all commercially available 4H-SiC wafers are manufactured using the modified Lely technique, referred to as the physical vapor transport (PVT) method [1]. Because the SiC crystal grows by the sublimation gas transported by the temperature difference between the SiC powder as the source material and the seed crystal, it is difficult to increase the growth rate of PVT. In particular, the growth rates of 0.1–2.0 mm/h have been reported [2-5], however, the crystals are usually grown at less than 0.5 mm/h because fast growth degrades the crystal quality in PVT. Such a low growth rate leads not only to higher wafer costs but also to higher energy consumption in manufacturing from heating the furnace for a long time.

Previously, we developed a high-temperature chemical vapor deposition (HTCVD) method as a high-speed crystal growth technique [6-8]. High-purity gases were used as source materials for HTCVD growth. Fast growth is realized via gas-flow transport of chemical species containing silicon and carbon to the seed crystal surface. As a result of crystal growth using seed crystals of 4 in or less, a growth rate of 3 mm/h or more was achieved while improving the crystal quality compared with

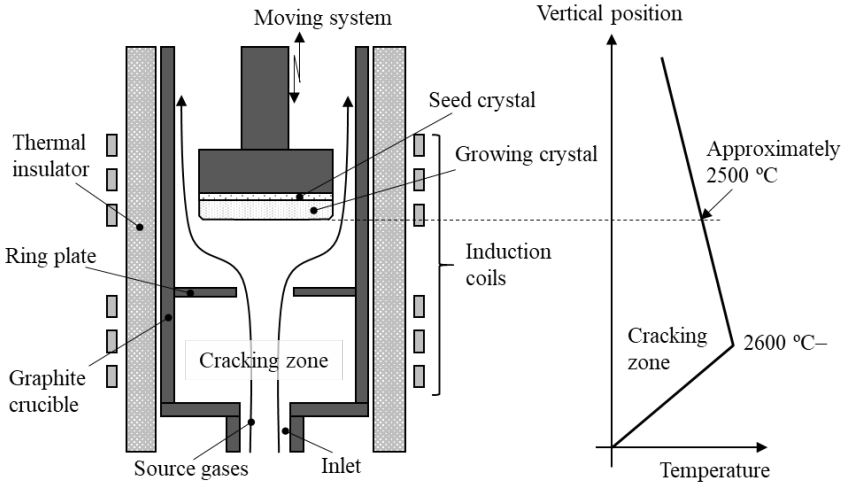

Fig. 1. Schematics of a high-temperature chemical vapor deposition (HTCVD) reactor and temperature distribution inside the reactor.

seed crystals [6, 7]. Although 150 mm 4H-SiC wafers have also been grown by HTCVD, the growth rate was only 0.5 mm/h [8]. To improve the productivity of 150 mm 4H-SiC wafers, an increase in the growth rate is required.

In this study, 150 mm 4H-SiC wafers were grown at over 1.5 mm/h with optimized furnace structure and growth conditions, and the quality of these wafers is discussed in comparison with previously reported PVT-grown crystals.

Crystal growth

The HTCVD reactor and its temperature distribution are illustrated in Fig. 1. The carbon crucible, covered with the thermal insulator, was heated using high-frequency induction coils. SiH_4 and C_3H_8 as source gases and H_2 as a carrier gas were introduced from the inlet at the bottom of the reactor and decomposed in a cracking zone maintained at temperatures above 2600 °C. The decomposed gas passed through the ring plate to control the gas flow and reached the seed crystal that was placed face down. The seed crystal was a 4H-SiC 4° off-axis C-face grown by PVT.

The crystal growth rate (GR) is expressed by the following formula:

$$GR = a\{P_{\mathrm{SiH_4}} - P_0(T_\mathrm{s})\}. \quad (1)$$

The growth rate is proportional to the difference between the SiH_4 input partial pressure $P_{\mathrm{SiH_4}}$ and equilibrium vapor pressure P_0 depending on the crystal surface temperature T_s. Hoshino *et al.* experimentally demonstrated that the growth rate increases with increasing vertical gas-flow velocity, even at the same SiH_4 partial pressure and surface temperature [9]. Tokuda *et al.* showed using thermal fluid simulation that the distribution of the growth rate in the crystal depends on the distribution of the vertical gas-flow velocity near the crystal surface [6]. These results suggest that the coefficient a depends on the vertical gas-flow velocity. Because the convex crystal generates a large thermal stress during cooling from approximately 2500 °C to room temperature and cracks occur in the grown crystal, it is essential to grow flat-shaped crystals [8]. These factors depend on the growth rate, except for the SiH_4 partial pressure, which varies slightly in the radial direction. Control of the in-plane distribution of temperature and flow velocity is thus important for fabricating a flat crystal shape. As the crystal diameter increases, the space in the reactor and the gas flow also increase, and the precise control of these parameters becomes difficult.

We designed the structure inside the reactor so that the in-plane temperature difference of the seed crystal surface was within 10 °C and the gas-flow velocity was uniform using thermal fluid simulation. The temperature of the crystal surface was controlled at 2490 °C. The SiH_4 partial pressure was

Fig. 2. Photograph of the 150 mm boule grown at 1.5 mm/h.

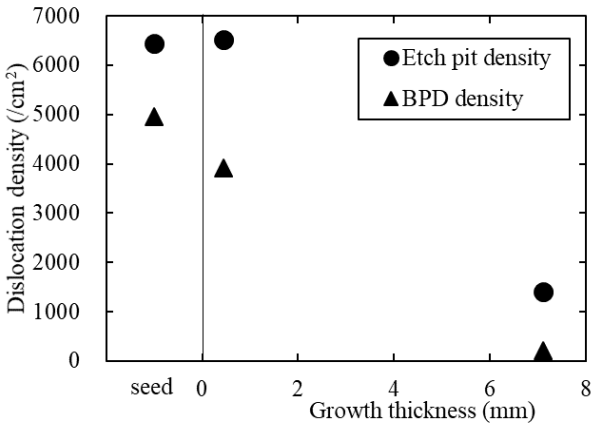

Fig. 3. Dislocation densities of wafers grown at 1.5 mm/h taken from seed and grown crystal, evaluated by molten KOH etching.

10.3 kPa. The growth rate was 1.5 mm/h, and the growth height was approximately 8 mm. A photograph of the grown 150 mm boule after cylindrical grinding is presented in Fig. 2.

Furthermore, the inner diameter and position of the ring plate were optimized to increase the vertical gas-flow rate to the crystal surface while maintaining the uniformity of the temperature and the vertical gas-flow rate on/near the surface. Although the surface temperatures and the flow rates of H_2, SiH_4, and C_3H_8 introduced from the inlet were the same as those for growth at 1.5 mm/h, the growth rate was increased to 2.0 mm/h by increasing the gas-flow velocity to the surface. The height of the grown crystal was approximately 8 mm.

Quality Evaluation of the 150 mm Substrates

The 4H-SiC wafers used for quality evaluation were sliced from the boule grown at 1.5 mm/h. These wafers were taken from the seed at the initial stage of the growth process and near the top of the boule. The wafer surfaces were polished using chemical mechanical polishing (CMP). The dislocation densities were measured after molten KOH etching. The crystal quality was evaluated by transmission X-ray topography (Rigaku, XRT-200CCM) with the diffraction condition of $\boldsymbol{g} = 11\bar{2}0$.

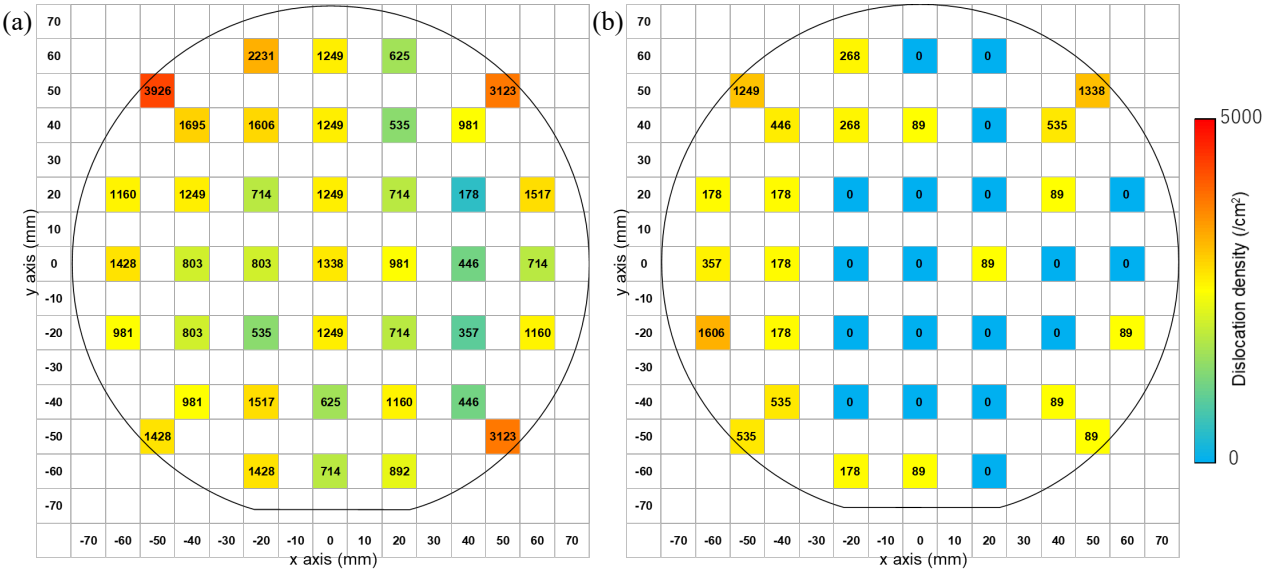

Fig. 4. Dislocation density distributions of the 150 mm wafer grown at 1.5 mm/h (growth thickness of 7.1 mm): (a) threading dislocations (TDs), (b) basal plane dislocations (BPDs).

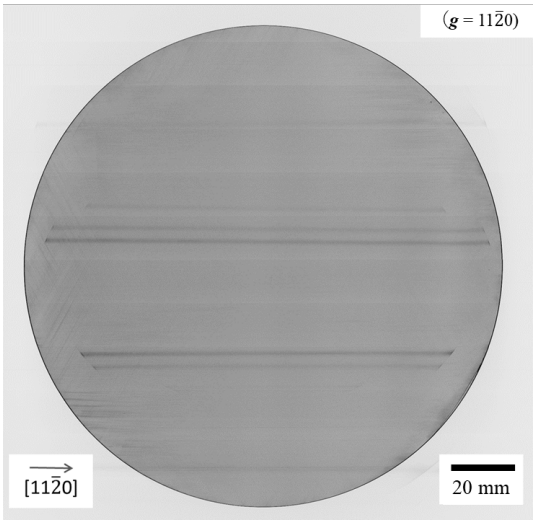

Fig. 5. X-ray topography image for the wafer grown at 1.5 mm/h (grown thickness of 7.1 mm).

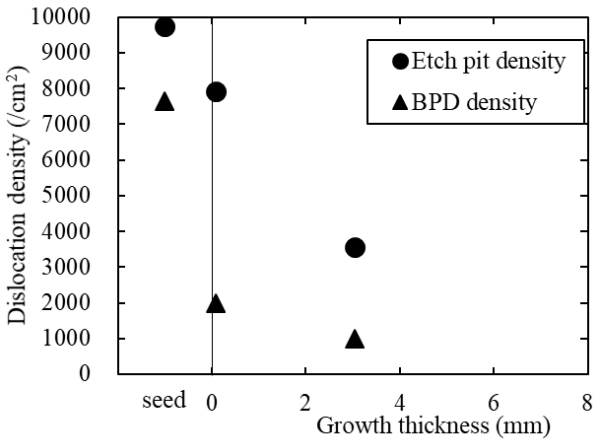

Fig. 6. Dislocation densities of wafers grown at 2.0 mm/h taken from seed and grown crystal.

Basal plane dislocation (BPD) densities and etch pit densities (total BPD density and threading dislocation (TD) density) of the wafers grown at 1.5 mm/h are graphically depicted in Fig. 3. The etch pit density was almost the same in the seed crystal and the initial growth stage; however, the BPD density at the initial stage was lower than that of the seed. The densities of the etch pit and BPD decreased significantly during the growth to 7.1 mm. The etch pit density and the BPD density of the grown crystal at the growth thickness of 7.1 mm were 1397 and 211 /cm^2, respectively.

Figure 4 displays the density distributions of the TDs and BPDs of the wafer grown at 1.5 mm/h (for growth thickness of 7.1 mm). BPDs near the center of wafer were less than 100 /cm^2; whereas, on the outer periphery, the densities of TDs and BPDs were slightly high. To obtain more detailed information on the dislocation distribution, this wafer was observed using X-ray topography (Fig. 5). Large defects such as polytypes and micropipes were not observed over the whole wafer. Additionally, a black linear contrast due to prismatic dislocations was observed in the outer periphery. This is considered to be the cause of the increase of dislocations in the periphery.

In addition, wafers obtained from the mid-growth and seed positions of the boule grown at 2.0 mm/h were evaluated using molten KOH. A comparison of Figs. 3 and 6 shows that a similar tendency was obtained, even when the growth rate was increased from 1.5 to 2.0 mm/h.

Discussion

As a result of the evaluation of the 150 mm wafer grown at over 1.5 mm/h using the HTCVD method, there was no increase in the dislocation density in the initial growth stage, and the dislocation density decreased during the growth to 7.1 mm. Here, we discuss the following two points in comparison with the reported results of PVT growth: (1) there is no increase in dislocation in the initial growth stage, and (2) the dislocation density decreases during growth.

(1) No increase in dislocations in the initial growth stage

A sharp increase in dislocations during the initial stage of PVT growth has been reported [10]. The dislocation density reached almost 100 times that of the seed dislocation density. These causes include an increase in the local nitrogen concentration, carbon inclusions, and treatment of the seed surface. First, an increase in nitrogen concentration was observed in the region of ~50 μm from the start of PVT growth; thus, dislocations were generated owing to lattice mismatch between the seed and the grown crystal depending on the nitrogen concentration [11]. However, in HTCVD growth, the generation of dislocations was suppressed through control of the flow rate of nitrogen during the

initial stage. Figure 7 shows that the distribution of the nitrogen concentration around the interface between the seed and the crystal grown by HTCVD was measured using secondary ion mass spectrometry. The nitrogen concentration decreased from approximately 12 to 8 × 10^{18} cm^{-3} across the interface. According to ref. 11, the nitrogen concentration at the interface increased from approximately 5 to 12 × 10^{18} cm^{-3} as a result of PVT growth under improved conditions. Therefore, the difference in nitrogen concentration between the seed and the initial stage of HTCVD is smaller than that of PVT. By adjusting the nitrogen flow rate at the initial stage in the future, it is possible to further reduce the nitrogen concentration difference at the interface. Second, carbon inclusions are responsible for the dislocations of large Burgers vectors, such as micropipes [12, 13]. Because the sublimation gas from the SiC powder had a higher partial pressure of Si than that of Si_2C and SiC_2 in PVT, the Si-rich gas degraded the side wall of the carbon crucible, and thus carbon inclusions were mixed in the growing crystal. Large quantities of carbon inclusions occur during the early stage of PVT growth [14]. In HTCVD, source gases with an arbitrarily controlled C/Si ratio can be supplied from the start to the end of the growth. To further suppress carbon inclusions, the inner wall of the carbon crucible was protected with inert materials that were resistant to gas etching. Finally, because the subsurface damage of the seed causes dislocations, the seed surface is polished by CMP before PVT growth [15]. However, the complete removal of subsurface damage is difficult even if the seed surface is polished by CMP. Meanwhile, in HTCVD, the seed surface is slightly etched by the hydrogen of the carrier gas before the growth starts, and the damaged layer is removed so that the generation of dislocations is suppressed. From the above discussion, the dislocation density in the initial stage did not increase in HTCVD, unlike PVT growth.

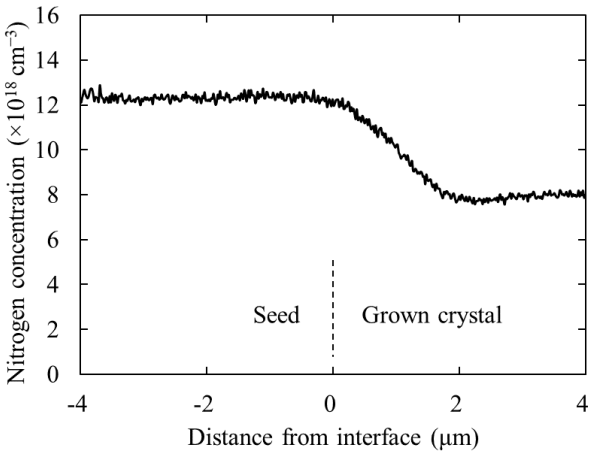

Fig. 7. Distribution of the nitrogen concentration around the interface between the seed and the grown crystal.

Figure 3 shows that the etch pit density at the initial growth stage was almost the same as that of the seed, but the BPD density at the initial stage was lower than that of the seed. The ratio of BPD density to etch pit density at the seed and the initial stage is 77% and 60%, respectively. BPDs convert to TDs at or very near the interface between the seed and grown crystal. At the growth front, the dislocation glides toward the surface under influence of the image force acting on the unit length of dislocation line [16]. In solution growth, TDs in the seed were converted into dislocations parallel to the basal plane by large steps [17]. As dislocations in the crystal grown by HTCVD converted from BPDs to TDs, the growth surface at the initial stage was assumed to comprise micro steps. Furthermore, the ratio of BPD density to etch pit density at the growth of 7.1 mm decreased to 15%. Previous studies have reported that macro-step bunching does not form at growth rates of less than 3 mm/h when the C/Si ratio is close to stoichiometry [7]. For growth of the 150 mm crystal, large steps notably did not occur even at the high growth rate of – 2.0 mm/h.

(2) Decrease in dislocation densities during HTCVD growth

BPDs can be generated by thermal stress in the grown crystal. The resolved shear stress on the basal plane (τ) is expressed as follows:

$$\tau = \sigma_{xx} \cdot \sin 4° \cos 4° = (\sigma_{rr} \cos^2 \theta + \sigma_{\theta\theta} \sin^2 \theta) \cdot \sin 4° \cos 4° \quad (2)$$

σ_{xx} is the resolved shear stress acting on the BPDs, σ_{rr} is the radial stress, $\sigma_{\theta\theta}$ is the circumferential stress, and θ is the azimuthal angle when the x direction is parallel to the step flow [17]. In our studies, the furnace configuration was controlled to reduce the temperature distribution in the crystal plane during growth at 1.5 mm/h. The standard deviation of the surface profile of the grown crystals was 0.48. For comparison, a convex crystal was prepared under conditions of different temperature distributions. The standard deviation of the surface profile was 0.96. Thus, the two crystals with different shapes were named flat and convex. The in-furnace structure and surface shape of each crystal were modeled, and the temperature distribution in the crystal was simulated. The radial temperature distributions in the crystals are displayed in Fig. 8. The in-plane temperature difference was 10 °C for the flat crystal and 28 °C for the convex crystal. The distributions of τ calculated from σ_{rr} and $\sigma_{\theta\theta}$ obtained from the simulation are presented in Fig. 9. The resolved shear stress on the basal plane of the convex crystal is larger than that of the flat crystal.

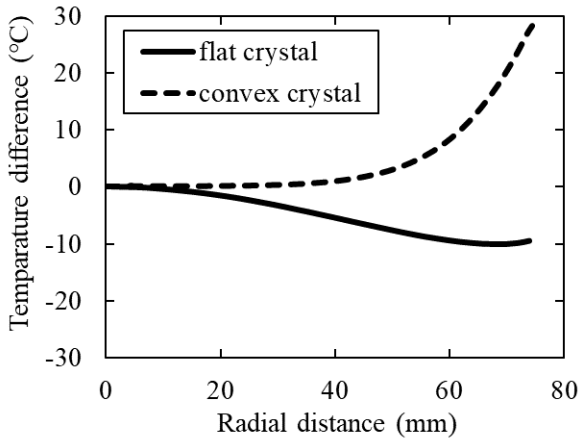

Fig. 8. Temperature differences from the centers of the flat crystal and the convex crystal.

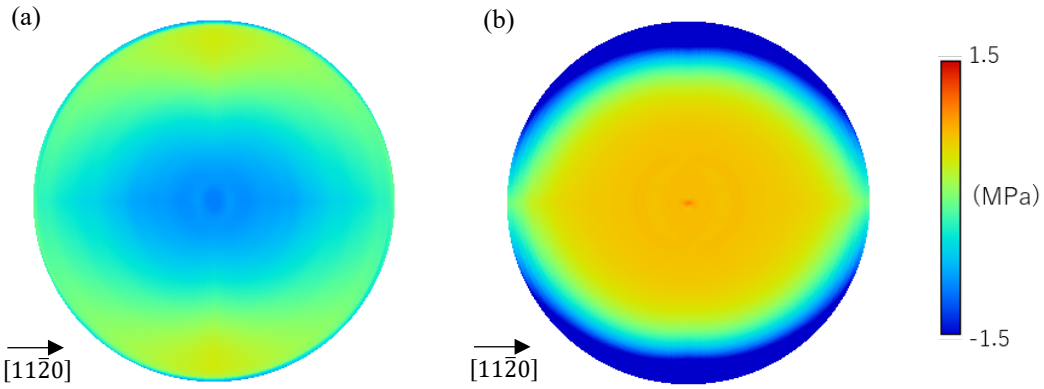

Fig. 9. Distributions of resolved shear stresses of (a) flat crystal and (b) convex crystal.

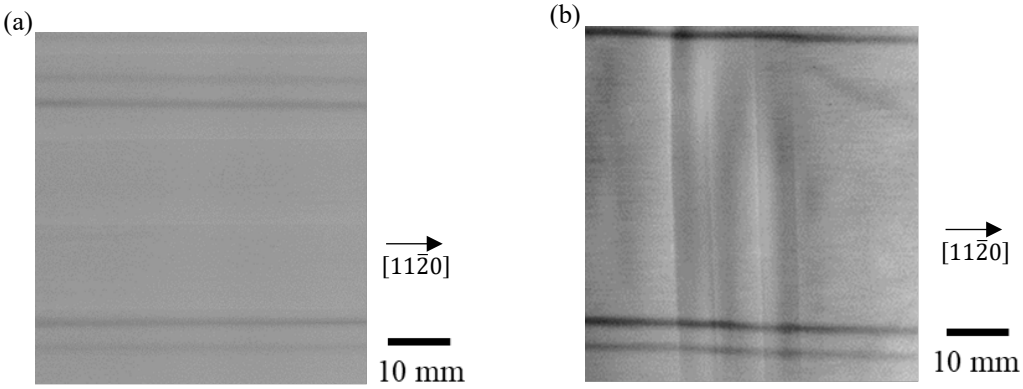

Fig. 10. X-ray topography images at the center regions of (a) flat crystal and (b) convex crystal.

Table 1. Densities of TDs and BPDs of the flat crystal and the convex crystal.

	TD density (/cm^2)	BPD density (/cm^2)
Flat crystal	1,186	211
Convex crystal	3,541	17,899

As a result of evaluating these wafers obtained from the two crystals by X-ray topography (Fig. 10), a strip-like black contrast extending in the longitudinal direction near the center of the wafer was observed in the convex crystal. This contrast was because of the BPD arrays. The dislocation densities of the crystals measured after molten KOH etching are presented in Table 1. On the convex crystal, approximately 18,000 BPDs were observed, on average, because of the generation of the BPD array. These results indicate that the increase in dislocation density was prevented by flattening the growth surface, realized via reduced temperature distribution of the growth surface.

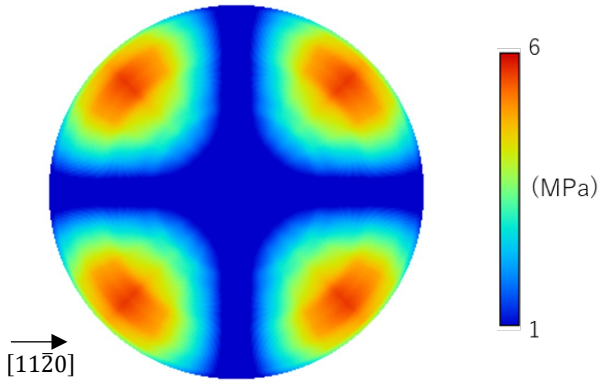

Fig. 11. Distribution of resolved shear stress of flat crystal grown at 1.5 mm/h for $(1\bar{1}00)[11\bar{2}0]$ prismatic slip system.

However, as reported by Guo *et al.* [18], three types of prismatic dislocations exist, all of which generate large resolved shear stresses at the outer periphery of the wafer. For prismatic system $(1\bar{1}00)[11\bar{2}0]$, the distribution of the resolved shear stress was calculated using the thermal fluid simulation results of the flat crystal, as shown in Fig. 11, where the magnitude exceeds 5 MPa at the outer periphery. The shear stress acting on the other two types of prismatic dislocations was also high in the outer area of the crystal. When the stress exceeded a certain value at which active dislocations glide, prismatic dislocations were introduced into the outer periphery of the wafer grown at 1.5 mm/h.

Next, we discuss the reason for the reduction in dislocations. The total dislocation density decreased from 6520 to 1397 during growth to 7.1 mm. Hoshino *et al.* reported that defect density was reduced during HTCVD growth using 2-in diameter seeds [19]. It was found that the dislocation density decreased with the growth of the 150 mm crystals. As a result of observing the cross section of the crystal grown by HTCVD using synchrotron radiation topography, the dislocation decreased by pair annihilation [20]. Because the crystal surface temperature in HTCVD was higher than that in PVT, the migration rate of dislocations was faster and pair annihilation was likely to occur. The dislocation was considerably reduced during growth to 7.1 mm.

Summary

In this work, 150 mm 4H-SiC wafers with low dislocation density were grown at more than 1.5 mm/h by HTCVD. The growth rate of 2.0 mm/h was achieved as the gas-flow velocity was increased. As a result of evaluating the wafer grown at 1.5 mm/h by molten KOH etching, an increase in dislocations in the initial growth stage was not observed compared with the seed crystal. The dislocation density decreased drastically during the growth to 7.1 mm. The reason why dislocations did not increase in the initial stage was discussed in comparison with PVT. It was demonstrated that an increase in nitrogen concentration, generation of carbon inclusion, and damage of the seed surface, which are causes of the initial dislocation increase in PVT, were insignificant based on the principle of crystal growth in HTCVD. The resolved shear stress, which causes the increase in dislocations during growth, was also calculated. In the flat-grown crystal, the resolved shear stress was small, and the dislocation did not increase. However, in the convex crystal, the BPD arrays were generated

because of the large shear stress, and the crystal quality deteriorated significantly. The decrease in dislocations was attributed to the frequent annihilation of dislocations caused by the growth at a high temperature compared with PVT. Because the gas-flow rate and gas ratio can be controlled in HTCVD, the generation of defects was suppressed. We demonstrated that high-quality 150 mm 4H-SiC wafers can be grown at over 1.5 mm/h using HTCVD.

References

[1] A.R. Powell, Industrial Perspectives of SiC Bulk Growth, in: P. Wellman, N. Ohtani and R. Rupp (Eds.), Wide Bandgap Semiconductors for Power Electronics, WILEY-VCH, Weinheim, 2022, pp.33-46.

[2] E.K. Sanchez, J.Q. Liu, M.D. Graef, M. Skowronski, W.M. Vatter and M. Dadley, J. Appl. Phys. 91 (2002) 1143.

[3] P. Wellmann, Z. Herro, A. Winnacker, R. Püsche, M. Hundhausen, P. Masri, A. Kulik, M. Bogdanov, S. Karpov, M. Ramm and Y. Makarov, J. Cryst. Growth 275 (2005) e1807.

[4] N. Ohtani, T. Fujimoto, M. Katsuno, T. Aigo and H. Yashiro, J. Cryst. Growth 237-239 (2002) 1180.

[5] T. Kimoto, Prog. Cryst. Growth Charact. Mater. 62 (2016) 329.

[6] Y. Tokuda, N. Hoshino, H. Kuno, H. Uehigashi, T. Okamoto, T. Kanda, N. Ohya, I. Kamata and H. Tsuchida, Mater. Sci. Forum 1004 (2020) 5.

[7] N. Hoshino, I. Kamata, Y. Tokuda, E. Makino, T. Kanda, N. Sugiyama, H. Kuno, J. Kojima and H. Tsuchida, J. Cryst. Growth 478 (2017) 9.

[8] T. Okamoto, T. Kanda, Y. Tokuda, N. Ohya, K. Betsuyaku, N. Hoshino, I. Kamata and H. Tsuchida, Mater. Sci. Forum 1004 (2020) 14.

[9] N. Hoshino, I. Kamata, Y. Tokuda, E. Makino, N. Sugiyama, J. Kojima and H. Tsuchida, Appl. Phys. Express 7 (2014) 065502.

[10] K. Tani, T. Fujimoto, K. Kamei, K. Kusunoki, K. Seki and T. Yano, Mater. Sci. Forum 858 (2016) 73.

[11] H. Suo, S. Tsukimoto, K. Eto, H. Osawa, T. Kato and H. Okumura, Jpn. J. Appl. Phys. 57 (2018) 065501.

[12] M. Dudley, X.R. Huang, W. Huang, A. Powell, S. Wang, P. Neudeck and M. Skowronski, Appl. Phys. Lett. 75 (1999) 784.

[13] D. Hofmann, E. Schmitt, M. Bickermann, M. Kölbl, P.J. Wellmann and A. Winnacker, Mater. Sci. Eng. B 61-62 (1999) 48.

[14] X. Xie, J. Yu, X. Yang, X. Chen, X. Xu, X. Hu, X. Liu and D. Liu, Mater. Sci. Forum 1004 (2020) 20.

[15] A.R. Powell, R.T. Leonard, M.F. Brady, St.G. Muller, V.F. Tsvetkov, R. Trussell, J.J. Sumakeris, H. McD. Hodgood, A.A. Burk, R.C. Glass and C.H. Carter, Mater. Sci. Forum 457-460 (2004) 41.

[16] S. Ha, P. Mieszkowski, M. Skowronski and L.B. Rowland, J. Cryst. Growth 244 (2002) 257.

[17] X. Zhang, M. Nagano and H. Tsuchida, Mater. Sci. Forum 679-680 (2011) 306.

[18] J. Guo, Y. Yang, B. Raghothamachar, J. Kim, M. Dudley, G. Chung, E. Sanchez, J. Quast and I. Manning, J. Electron. Mater. 46 (2017) 2040.

[19] N. Hoshino, I. Kamata, T. Kanda, Y. Tokuda, H. Kuno and H. Tsuchida, Appl. Phys. Express 13 (2020) 095502.

[20] I. Kamata, N. Hoshino, K. Betsuyaku, T. Kanda and H. Tsuchida, J. Cryst. Growth 590 (2022) 126676.